Temperature dependence of spin pumping in YIG/NiO(x)/W multilayer

Lijun Ni(倪丽君)[1], Wenqiang Wang(王文强)[1], Lichuan Jin(金立川)[2], Jiandong Ye(叶建东)[1], Hehe Gong(巩贺贺)[1], Xiang Zhan(战翔)[3], Zhendong Chen(陈振东)[4], Longlong Zhang(张龙龙)[1], Xingze Dai(代兴泽)[1], Yao Li(黎遥)[1], Rong Zhang(张荣)[1], Yi Yang(杨燚)[1], Huaiwu Zhang(张怀武)[2], Ronghua Liu(刘荣华)[3], Lina Chen(陈丽娜)[5,†], and Yongbing Xu(徐永兵)[1,6,‡]

[1] *Jiangsu Provincial Key Laboratory of Advanced Photonic and Electronic Materials, School of Electronic Science and Engineering, Nanjing University, Nanjing* 210093, *China*

[2] *State Key Laboratory of Electronic Thin Films and Integrated Devices, University of Electronic Science and Technology of China, Chengdu* 610054, *China*

[3] *Jiangsu Provincial Key Laboratory for Nanotechnology, School of Physics, Nanjing University, Nanjing* 210093, *China*

[4] *Jiangsu Key Laboratory of Opto-Electronic Technology, Center for Quantum Transport and Thermal Energy Science, School of Physics and Technology, Nanjing Normal University, Nanjing* 210023, *China*

[5] *School of Science, Nanjing University of Posts and Telecommunications, Nanjing* 210023, *China*

[6] *York–Nanjing Joint Centre for Spintronics and NanoEngineering, Department of Electronic Engineering, University of York, York YO*10 5*DD, United Kingdom*

(Received 5 January 2022; revised manuscript received 15 March 2022; accepted manuscript online 1 April 2022)

We report the temperature dependence of the spin pumping effect for $Y_3Fe_5O_{12}$ (YIG, 0.9 μm)/NiO (t_{NiO})/W (6 nm) (t_{NiO} = 0 nm, 1 nm, 2 nm, and 10 nm) heterostructures. All samples exhibit a strong temperature-dependent inverse spin Hall effect (ISHE) signal I_c and sensitivity to the NiO layer thickness. We observe a dramatic decrease of I_c with inserting thin NiO layer between YIG and W layers indicating that the inserting of NiO layer significantly suppresses the spin transport from YIG to W. In contrast to the noticeable enhancement in YIG/NiO ($t_{NiO} \approx$ 1–2 nm)/Pt, the suppression of spin transport may be closely related to the specific interface-dependent spin scattering, spin memory loss, and spin conductance at the NiO/W interface. Besides, the I_c of YIG/NiO/W exhibits a maximum near the T_N of the AF NiO layer because the spins are transported dominantly by incoherent thermal magnons.

Keywords: spin pumping effect, spin transport, charge current I_c, linewidth ΔH, temperature dependence

PACS: 85.75.–d, 75.75.Cd, 72.25.Mk, 32.30.Dx **DOI:** 10.1088/1674-1056/ac6333

With the development of spintronics, the generation and detection of spin current have become a topic of concern. Meanwhile, the controllable modulation of the spin transport of electrons is also central to fabricating robust spintronics devices.[1–5] Spin transport in ferromagnetic (FM) and nonmagnetic materials (NM) has been extensively studied. Pure spin current can be pumped from FMs into NMs by ferromagnetic resonance (FMR) spin pumping[6,7] or a thermal gradient.[8,9] Furthermore, the pure spin current can be converted into the charge current I_c by the ISHE due to bulk and interfacial spin–orbit coupling at the NM and FM/NM interface,[10] thereby realizing the electrical detection of pure spin current. So, the effective modulation of spin current injection and the spin transport plays an important role for the impact on I_c in FM/NM heterostructures.

Recently, spin current studies, especially spin transport, have been expanded into the antiferromagnetic (AF) materials, e.g., NiO, IrMn, and Fe_2O_3.[11–15] For instance, NiO is a well-known AF insulator with a bulk Néel temperature of T_N = 525 K.[16] And the characteristic frequency of AF NiO is up to 1 THz in magnetic resonance measurements, which is attractive for developing THz devices.[17] Surprisingly, the unexpected enhancement of spin transport via inserting thin AF NiO between an FM (such as YIG) and Pt was discovered in FMR spin pumping and spin Seebeck experiments.[9,12,18,19] The spin transport in the AFs is optimal at a temperature near the AF Neél temperature T_N, suggesting that the spin transport through the AF insulators is related to AF magnons and strong spin fluctuations near T_N.[7,9] In addition, Hammel *et al.*[20] found that the transport efficiency of spin current J_s was reduced at room temperature, when a Cu layer was inserted between YIG and Pt in FMR spin pumping experiment. While the insertion of a similar Cu interlayer between YIG and W improves the spin current J_s injection into W. Therefore, it is interesting how spin transport is affected if the NiO interlayer is inserted between YIG and W. In fact, Chien *et al.* have reported that 1-nm thin NiO suppressed the spin current pumped into W from YIG in the Seebeck effect experiment only measured at room temperature.[9] Hence, it is necessary to systematically explore the effect of temperature on spin transport between YIG and W with different NiO interlayer thickness. However, very few studies have been reported on this topic so

[†]Corresponding author. E-mail: chenlina@njupt.edu.cn
[‡]Corresponding author. E-mail: ybxu@nju.edu.cn

© 2022 Chinese Physical Society and IOP Publishing Ltd

far.

So, we systematically explore the effect of temperature on spin transport between YIG and W with different NiO interlayer thicknesses. We chose YIG/NiO (t_{NiO})/W (6 nm) (t_{NiO} = 0 nm, 1 nm, 2 nm, and 10 nm) stacked structure and focused on the FMR spin-pumping-induced charge current I_c over a wide temperature range (30–300 K). The transmitted spin current detected by ISHE in the W had a maximum near the T_N of the AF NiO layers, consistent with the previous reports in the YIG/NiO/Pt system. On the contrary, we found that 1 nm thick NiO is enough to significantly suppress spin transport between YIG and W by varying NiO thickness, indicating that interfaces in YIG/NiO/W heterostructures play a vital role in the spin transmission except for magnetic fluctuation of the AF NiO spacer.

The 0.9-μm thick YIG films were grown on $Gd_3Ga_5O_{12}$ (GGG, (111)) substrates by liquid-phase epitaxy. The YIG samples were degreased via ultrasonic bathing in acetone and ethyl alcohol for 12 min and cleaned by deionized water, before being placed into the deposition chamber. Then, we used ultrahigh vacuum magnetron sputtering with a base pressure of 3×10^{-8} Torr to fabricate the YIG (0.9 μm)/NiO (t_{NiO})/W (6 nm) (t_{NiO} = 0 nm, 1 nm, 2 nm, and 10 nm) samples at room temperature. The reactive (Ar+O_2) pressure for NiO deposition was 4.5×10^{-3} Torr. And the working Ar pressure was 5×10^{-3} Torr for W deposition. Finally, all samples were patterned into a 4.0-mm long and 0.5-mm wide small rectangular bar by combining optical lithography and ion Ar+ plasma etching. The FMR spin pumping measurements of YIG (0.9 μm)/NiO (t_{NiO})/W (6 nm) (t_{NiO} = 0 nm, 1 nm, 2 nm, and 10 nm) samples were performed by using the coplanar waveguides (CPW) method over the temperature range from 300 K to 30 K, and the microwave frequency (f) and power (P_{rf}) were set to be 9 GHz and 20 dBm, respectively. As illustrated in the schematic diagrams shown in Fig. 1(a), the external bias magnetic field H was applied along the x-axis, and voltage measurements were performed along the y-axis. At YIG resonance, the precessing YIG magnetization excites the AF moments at YIG/NiO interface. The AF magnons or fluctuations in NiO carry the angular momentum (a vertical spin current J_s) through the NiO thickness to the NiO/W interface, where the angular momentum is transferred across the NiO/W interface to the conduction electrons in the metal layer W along the z-axis with the spin polarization along the x-axis. Then, J_s in W can be converted to a charge current I_c via ISHE.

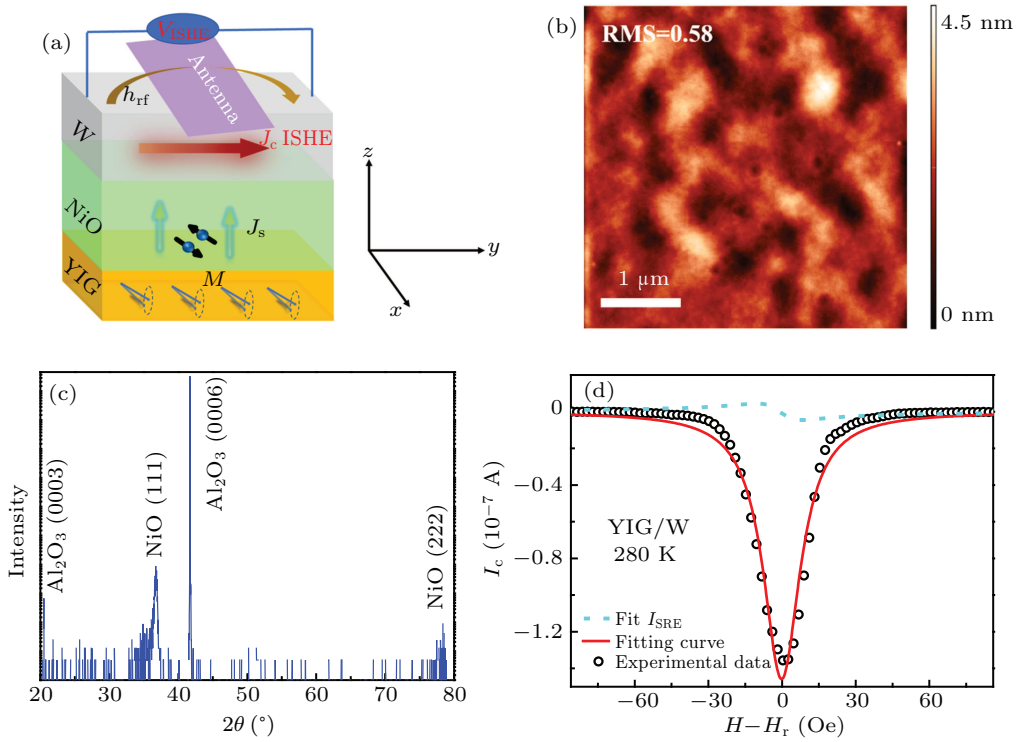


Fig. 1. (a) Schematic of the spin pumping and ISHE measurement with in-plane field H, (b) the atomic force microscopy images of the 0.9-μm bare YIG over an area of 4 μm×4 μm, (c) XRD spectrum of a 400 nm-NiO film, (d) fitting of the experimental data of I_c and the antisymmetric component for YIG/W at 280 K.

Atomic force microscopy (AFM) measurement shown in Fig. 1(b) reveals a root-mean-square (RMS) roughness of 0.58 nm for bare YIG, demonstrating the smooth surface of YIG film. High-resolution x-ray diffraction (XRD) scan of the 400-nm thick NiO film deposited on the c-plane sapphire substrates is presented in Fig. 1(c). Only (111) and (222) peaks of NiO film are detected, indicating that the NiO films are of high quality with a preferred orientation along ⟨111⟩. As plotted in Fig. 1(d), we fit a typical charge current I_c curve of the YIG/W

sample at 280 K by the expression as follows:[19]

$$I_c = S\frac{W^2}{\left[(H-H_r)^2+W^2\right]} - A\frac{W(H-H_r)}{\left[(H-H_r)^2+W^2\right]}, \quad (1)$$

where S is the symmetric part of the voltage amplitude, which corresponds mainly to the voltage coming from ISHE, and A is the antisymmetric part, which originates from spin rectification effect (SRE), respectively. The W is half of the resonance linewidth ΔH. The H_r represents the resonance field. The asymmetric signal I_{SRE} is negligible, and the symmetric Lorentzian shape can mainly fit the experimental I_c curve.

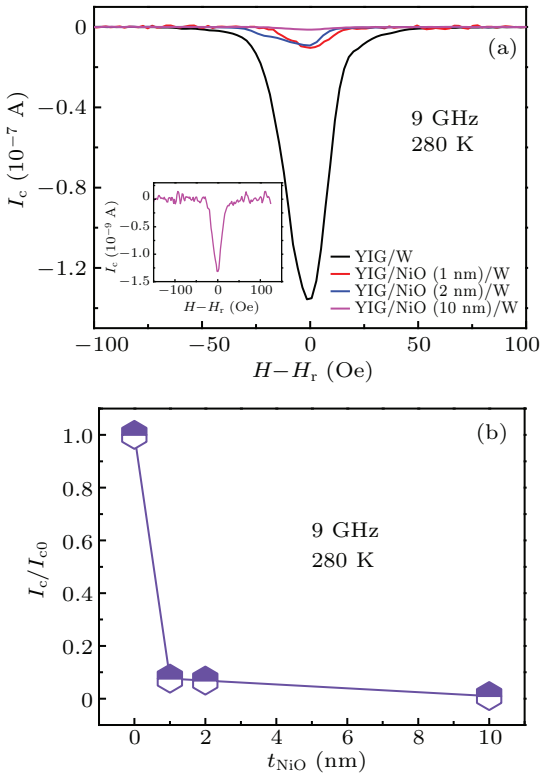


Fig. 2. (a) The I_c vs. $H-H_r$ spectra derived from FMR spin pumping voltage measurements for the YIG/NiO (t_{NiO})/W (6 nm) samples with t_{NiO} of 0 nm,1 nm, 2 nm, and 10 nm. The inset in (a) only shows the magnetic field dependence of the I_c for the sample with $t_{NiO} = 10$ nm. (b) At $T = 280$ K and $f = 9$ GHz, normalized charge current I_c/I_{c0} as a function of the NiO thickness.

Figure 2(a) shows that the charge current I_c (I_{c0}) vs. $H-H_r$ (H_r is the resonance field of YIG) spectra for YIG/NiO (t_{NiO})/W ($t_{NiO} = 0$ nm, 1 nm, 2 nm, and 10 nm) samples at $T = 280$ K, and $f = 9$ GHz. The I_{c0} of the YIG/W sample at the FMR point is 0.136 μA. When a 1-nm thick NiO interlayer is inserted between the YIG and W, we observe a decrease of the I_c at the FMR point by one order of magnitude relative to the YIG/W bilayer. Contrary to the previously reported enhancement of J_s in YIG/NiO/Pt and Ta systems,[9] 1-nm inserting layer NiO can dramatically suppress the spin current transmission in the YIG/NiO/W system. Besides, note that although the I_c becomes much smaller for the 10-nm thickness of NiO [the inset of Fig. 2(a)], an obvious I_c signal can still be well detected. Spin current J_s smoothly transmitting across the insulator NiO of 10-nm thick film implies that the insulating AF NiO spacer layer has a good spin transmission, consistent with the previous spin transports of NiO. To more intuitively present the variation trend of I_c generated at the FMR point with NiO thickness, we compare the relative magnitudes of I_c among the samples with three different NiO thicknesses. As displayed in Fig. 2(b), the I_c in YIG/NiO/W trilayers normalized to I_{c0} in YIG/W bilayer shows a gradual decrease with increasing NiO thickness except for the dramatical drop of I_c/I_{c0} from 1 to 0.08 at $t = 1$ nm. The significant suppression of the spin current transmission in the studied YIG/NiO/W system, in contrast to previously reported enhancement in YIG/NiO ($t_{NiO} \approx$ 1–2 nm)/Pt and Ta systems, should be closely related to these interfacial effects (e.g., interfacial spin scattering, spin memory loss, and spin conductance) caused by inserting NiO layer rather than the bulk spin transport in the NiO layer.[9,20,21]

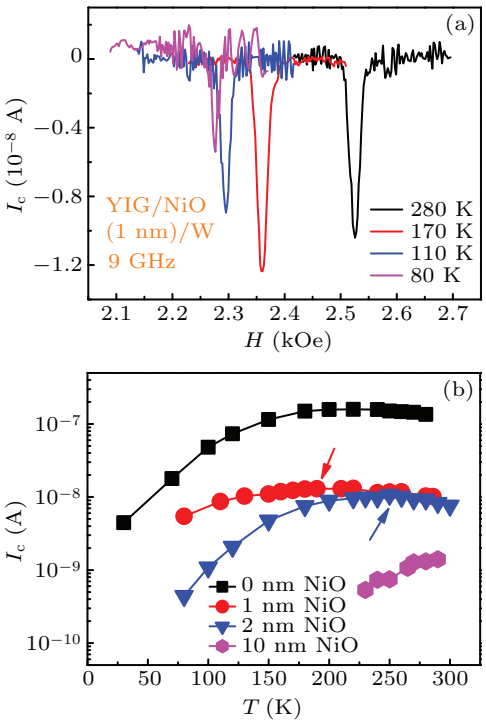


Fig. 3. (a) At $f = 9$ GHz, the magnetic field dependence of the I_c for the YIG/NiO (1 nm)/W sample with different temperatures, (b) the temperature dependences of the I_c for the YIG/NiO (t_{NiO})/W samples with t_{NiO} from 0 to 10 nm. The peak value T_M of YIG/NiO (t_{NiO})/W samples with $t_{NiO} = 1$ nm and 2 nm indicated by arrows.

We further study the temperature effect on spin transport of those four YIG/NiO (t_{NiO})/W ($t_{NiO} = 0$ nm, 1 nm, 2 nm, and 10 nm) samples. As we all know, due to finite size effects, the intrinsic Néel temperature T_N (t_{NiO}) of the isolated thin NiO layer is reduced with decreasing NiO thickness.[22,23] The previous reports found the T_N of 1–2 nm NiO film (T_N(1 nm) $\approx$ 170 K, T_N(2 nm) $\approx$ 260 K and T_N(10 nm) $>$ 300 K).[9,24,25] And, 280 K (near the room temperature) mentioned above is higher than the T_N of 1–2 nm NiO film. It is expected that

spin pumping may be strongly affected around T_N of the AF NiO for YIG/NiO/W system. Therefore, in the following, we perform FMR spin pumping measurements over a wide temperature range from 30 K to 300 K to explore temperature-dependent spin pumping signals I_c. Figure 3(a) shows the representative results of H vs. I_c spectra for the YIG/NiO (1 nm)/W sample with various temperatures of 80 K, 110 K, 170 K, and 280 K, respectively. Instead of a monotonic trend, the I_c seemingly exhibits a broad maximum at around 170 K [Fig. 3(b)]. Besides, H_r decreases with decreasing temperature due to the increase of the YIG magnetization and the exchange coupling effect between YIG and NiO with decreasing temperature.

Temperature dependences of I_c at the FMR point for all four YIG/NiO (t_{NiO})/W ($t_{NiO} = 0$ nm, 1 nm, 2 nm, and 10 nm) samples are extracted and summarized in Fig. 3(b). As shown in Fig. 3(b), all YIG/NiO/W samples are strong temperature-dependent and sensitive to the NiO layer thickness. Temperature dependence of ISHE signal I_c of YIG/NiO/W trilayers exhibits a maximum at a temperature T_M. The T_M is comparable to the reduced T_N (t_{NiO}) of NiO free film. The observed T_M for $t_{NiO} = 1$ nm and 2 nm samples are at 190 K and 250 K, respectively. And the T_M increases monotonically with the NiO thickness, consistent with the previously reported magnetic properties of NiO thin films. We note that the studied 10-nm NiO sample exhibits monotonical increases up to our highest accessible temperature of 300 K, suggesting a peak above RT. This is consistent with the 10-nm thick NiO film with a high T_N above RT. These similar temperature-dependent behaviors with an enhancement of I_c near T_N have been observed in YIG/NiO/Pt.[9] And Our FMR spin pumping experiments are carried out with the radio-frequency. So, these phenomena demonstrate that in antiferromagnetic insulators, the spins are transported dominantly by incoherent thermal magnons rather than coherent THz AFM dynamics.[7,9,26–28] In addition, our experimental results in Fig. 3(b) show that I_c is strongly suppressed towards lower temperatures. From Figs. 2(a) and 3(b), although 1–2 nm NiO is a paramagnetic insulator at high temperatures above T_N, there are still obvious ISHE signal I_c. The reason is that thermal magnons continuously evolve into thermal spin fluctuations, which would transport J_s at high temperatures above T_N.[7,9] We want to emphasize that, in the whole range of experimental temperatures, inserting the thin NiO layer (even 1-nm thick) always suppresses the spin transport from YIG to W layer in YIG/NiO/W trilayer systems, as the same with the above discussed for the results obtained at RT (280 K). It is unlike the YIG/NiO (1–2 nm)/Pt system reported previously, where the enhancement of injected spin current occurs. As for YIG/W bilayer, the overall decreasing trend of I_c is primarily ascribed to the increase of the magnetic damping $\alpha_{YIG/W}$ with decreasing temperature. And the spin relaxation attributed to rare-earth ions induces a reduction in spin pumping efficiency. The previously reported the moderate dependence of M_s of YIG, spin Hall angle θ_{SH} and the spin diffusion length λ_{SD} of W on temperature are not dominant factors for the decreasing behavior of I_c with temperature decreasing.[29–32]

The spin pumping experiments can further get the linewidth ΔH of the magnetization dynamics for the studied multilayers. Figure 4 displays the experimental ΔH as a function of temperature for the YIG/NiO (t_{NiO})/W samples with $t_{NiO} = 0$ nm, 1 nm and 10 nm at $f = 9$ GHz. We found that the ΔH of the YIG/W has a slight decrease from 280 K down to approximately 120 K, and then dramatically increases with decreasing temperature. In general, the linewidth ΔH (full width at half maximum) can be described by the following equation:[30,34]

$$\Delta H = \Delta H_{inh} + \frac{4\pi f \alpha}{\gamma}, \tag{2}$$

where ΔH_{inh} is the inhomogeneous broadening, and independent of the resonance frequency f. The temperature dependence of the linewidth ΔH can indirectly reflect temperature-dependent magnetic damping α. In general, the ΔH_{inh} arises from magnetic inhomogeneities owing to local variations of the magnetization and anisotropy constants, and their strong temperature dependences will lead to the increase of ΔH_{inh}, particularly at low temperature.[32,35,36] In addition, the strong temperature-dependent damping from rare-earth ion of YIG causes a significant increase of the linewidth ΔH in previous reports.[32,33] The enhancement of ΔH due to inhomogeneity is supposed to be small compared with that of rare-earth ions. As for the YIG/NiO (t_{NiO})/W ($t_{NiO} = 1$ nm, and 10 nm) samples, our results in Fig. 4 show that the ΔH stays almost invariant from about room temperature to the temperature (125 K for 1 nm and 225 K for 10 nm) at which the signal I_c disappears, indicating that the YIG/NiO exchange coupling induced-extra damping is small during temperature range of 300–125 K.[18,19]

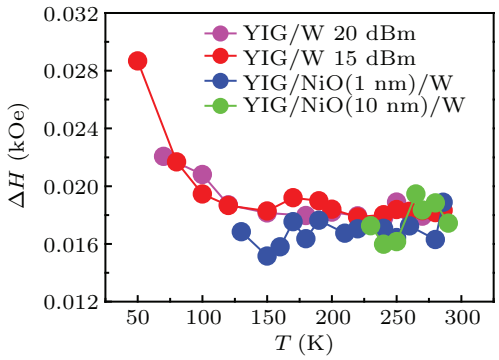


Fig. 4. Temperature dependences of the ΔH for the YIG/NiO (t_{NiO})/W samples with $t_{NiO} = 0$ nm (red and pink circles), 1 nm (blue triangle), and 10 nm (green diamond) at $f = 9$ GHz.

In summary, we have investigated the variation of ISHE signal I_c YIG (0.9 μm)/NiO (t_{NiO})/W (6 nm) ($t_{NiO} = 0$ nm, 1 nm, 2 nm, 10 nm) in a broad temperature range 300–30 K by utilizing the FMR spin pumping method. The value of I_c for YIG/NiO/W samples exhibits a broad maximum at the temperature T_M near the Néel temperature of NiO, suggesting that spin magnons of the insulating AF NiO dominate its spin transport. The I_c exhibits a obvious decrease over the entire experimental temperature range when the NiO layer is inserted between YIG and W. And the significant suppression of the spin current transmission in the YIG/NiO ($t_{NiO} = 1$ nm, 2 nm)/W system is in sharp contrast to the enhancement in YIG/NiO ($t_{NiO} \approx 1$–2 nm)/Pt and Ta systems, suggesting the interfacial effects of NiO/W (e.g., interfacial spin scattering, spin memory loss, and spin conductance) dominate spin transport rather than the bulk NiO layer with a low spin loss. Our results reveal that the amplification or inhibition of spin transport in various magnetic heterostructures closely depends on the specific interface-related materials.

Acknowledgements

We acknowledge support from the National Natural Science Foundation of China (Grant Nos. 11774160, 61427812, 61805116, 12004171, 61774081, and 62171096), the Natural Science Foundation of Jiangsu Province of China (Grant No. BK20192006), the National Key Scientific Instrument and Equipment Development Project of China (Grant No. 51827802), the Natural Science Foundation of Jiangsu Province of China (Grant Nos. BK20180056 and BK20200307), the Applied Basic Research Programs of the Science and Technology Commission Foundation of Jiangsu Province, China (Grant No. BK20200309), the Open Research Fund of Jiangsu Provincial Key Laboratory for Nanotechnology, the Scientific Foundation of Nanjing University of Posts and Telecommunications (NUPTSF) (Grant No. NY220164), and the State Key R&D Project of Guangdong, China (Grant No. 2020B010174002).

References

[1] Žutić I, Fabian J and Das Sarma S 2004 *Rev. Mod. Phys.* **76** 323
[2] Tserkovnyak Y, Brataas A, Bauer G E W and Halperin B I 2005 *Rev. Mod. Phys.* **77** 1375
[3] Kovalev A A, Brataas A and Bauer G E W 2002 *Phys. Rev. B* **66** 224424
[4] Tserkovnyak Y, Brataas A and Bauer G E W 2002 *Phys. Rev. Lett.* **88** 117601
[5] Sánchez J C R, Vila L, Desfonds G, Gambarelli S, Attané J P, Teresa J M D, Magén C and Fert A 2013 *Nat. Commun.* **4** 2944
[6] Wang H L, Du C H, Pu Y, Adur R, Hammel P C and Yang F Y 2013 *Phys. Rev. B* **88** 100406(R)
[7] Qiu Z, Li J, Hou D, Arenholz E, N'Diaye A T, Tan A, Uchida K I, Sato K, Okamoto S, Tserkovnyak Y, Qiu Z Q and Saitoh E 2016 *Nat. Commun.* **7** 12670
[8] Kikkawa T, Shen K, Flebus B, Duine R A, Uchida K, Qiu Z Y, Bauer G E W and Saitoh E 2016 *Phys. Rev. Lett.* **117** 207203
[9] Lin W W, Chen K, Zhang S F and Chien C L 2016 *Phys. Rev. Lett.* **116** 186601
[10] Zhu L, Ralph D C and Buhrman R A 2019 *Phys. Rev. Lett.* **122** 077201
[11] Moriyama T, Takei S, Nagata M, Yoshimura Y, Matsuzaki N, Terashima T, Tserkovnyak Y and Ono T 2015 *Appl. Phys. Lett.* **106** 162406
[12] Wang H L, Du C H, Hammel P C and Yang F Y 2015 *Phys. Rev. B* **91** 220410(R)
[13] Frangou L, Oyarzún S, Auffret S, Vila L, Gambarelli S and Baltz V 2016 *Phys. Rev. Lett.* **116** 077203
[14] Lebrun R, Ross A, Bender S A, Qaiumzadeh A, Baldrati L, Cramer J, Brataas A, Duine R A and Kläui M 2018 *Nature* **561** 222
[15] Hou D Z, Qiu Z Y and Saitoh E 2019 *NPG Asia Mater.* **11** 35
[16] Palmberg P W, DeWames R E and Vredevoe L A 1968 *Phys. Rev. Lett.* **21** 682
[17] Kampfrath T, Sell A, Klatt G, Pashkin A, Mährlein S, Dekorsy T, Wolf M, Fiebig M, Leitenstorfer A and Huber R 2010 *Nat. Photon.* **5** 31
[18] Wang H L, Du C H, Hammel P C and Yang F Y 2014 *Phys. Rev. Lett.* **113** 097202
[19] Jin L C, Jia K C, Zhang D N, Liu B, Meng H, Tang X L, Zhong Z Y, Zhang H W 2019 *ACS Appl. Mater. Interfaces* **11** 35458
[20] Du C H, Wang H L, Yang F Y and Hammel P C 2014 *Phys. Rev. Appl.* **1** 044004
[21] Liu L, Pai C F, Li Y, Tseng H W, Ralph D C and Buhrman R A 2012 *Science* **336** 555
[22] Alders D, Tjeng L H, Voogt F C, Hibma T, Sawatzky G A, Chen C T, Vogel J, Sacchi M and Iacobucci S 1998 *Phys. Rev. B* **57** 11623
[23] Ambrose T and Chien C L 1996 *Phys. Rev. Lett.* **76** 1743
[24] Liu Z Y and Adenwalla S 2003 *J. Appl. Phys.* **94** 1105
[25] Baruth A, Adenwalla S 2008 *Phys. Rev. B* **78** 174407
[26] Cheng Y, Zarzuela R, Brangham J T, Lee A J, White S, Hammel P C, Tserkovnyak Y and Yang F Y 2019 *Phys. Rev. B* **99** 060405
[27] Ohnuma Y, Adachi H, Saitoh E and Maekawa S 2014 *Phys. Rev. B* **89** 174417
[28] Takei S, Moriyama T, Ono T and Tserkovnyak Y 2015 *Phys. Rev. B* **92** 020409
[29] Wang H L, Du C H, Pu Y, Adur R, Hammel P C and Yang F Y 2014 *Phys. Rev. Lett.* **112** 197201
[30] Jungfleisch M B, Chumak A V, Kehlberger A, Lauer V, Kim D H, Onbasli M C, Ross C A, Kläui M and Hillebrands B 2015 *Phys. Rev. B* **91** 134407
[31] Okuno T, Taniguchi T, Kim S, Baek S C, Park B, Moriyama T, Kim K and Ono T 2016 *Jpn. J. Appl. Phys.* **55** 080308
[32] Shigematsu E, Ando Y, Ohshima R, Dushenko S, Higuchi Y, Shinjo T, Bardeleben H J v and Shiraishi M 2016 *Appl. Phys. Express* **9** 053002
[33] Seiden P E 1964 *Phys. Rev.* **133** A728
[34] Wang H L, Du C H, Hammel P C and Yang F Y 2014 *Appl. Phys. Lett.* **104** 202405
[35] Platow W, Anisimov A N, Dunifer G L, Farle M and Baberschke K 1998 *Phys. Rev. B* **58** 5611
[36] Martín-Rio S, Pomar A, Balcells Ll, Bozzo B, Frontera C and Martínez B 2020 *J. Magn. Magn. Mater.* **500** 166319